The American Journal of Pathology, Vol. 180, No. 5, May 2012

DOI: 10.1016/j.ajpath.2012.01.020

Gastrointestinal, Hepatobiliary, and Pancreatic Pathology

Enhanced Expression of Fibroblast Growth Factor Receptor 2 IIIc Promotes Human Pancreatic Cancer Cell Proliferation

Toshiyuki Ishiwata,* Yoko Matsuda,* Tetsushi Yamamoto,* Eiji Uchida,† Murray Korc,‡ and Zenya Naito*

From the Departments of Pathology and Integrative Oncological Pathology and Surgery for Organ and Biological Regulation,† Graduate School of Medicine, Nippon Medical School, Tokyo, Japan; and the Departments of Medicine and Biochemistry and Molecular Biology,‡ Indiana University School of Medicine and the Melvin and Bren Simon Cancer Center, Indianapolis, Indiana*

In pancreatic ductal adenocarcinoma (PDAC), the fibroblast growth factor receptor 1 (FGFR-1) IIIb isoform correlates with the inhibition of cancer cell proliferation, migration, and invasion, whereas FGFR-1 IIIc enhances cancer cell proliferation. The FGFR-2 IIIb isoform is expressed in PDAC, and its expression correlates with increased venous invasion. We examined the role of FGFR-2 IIIc in PDAC. FGFR-2 IIIc was expressed in all six pancreatic cancer cell lines examined and was highest in PANC-1 cells. FGFR-2 IIIc was abundant in the cancer cells from 83 of 117 PDAC cases, which correlated with decreased duration to development of liver metastasis after surgery. FGFR-2 IIIc-transfected cells exhibited increased proliferation *in vitro* and formed larger subcutaneous and orthotopic tumors, the latter producing more liver metastases. Moreover, FGF-2 exerted a more rapid stimulatory effect on the levels of phosphorylated extracellular signal-regulated kinase (p-ERK) in FGFR-2 IIIc stably transfected PANC-1 cells, compared with control cells. FGFR-2 IIIc-transfected cells also formed more spheres and contained more side population cells. Suppression of FGFR-2 IIIc expression inhibited the proliferation of PANC-1 cells, whereas an anti-FGFR-2 IIIc antibody inhibited the proliferation and migration of PANC-1 cells. Thus, high FGFR-2 IIIc levels in PDAC contribute to disease aggressiveness and confer to pancreatic cancer cells features suggestive of cancer stem cells, indicating that FGFR-2 IIIc may be a novel and important therapeutic target in PDAC. ***(Am J Pathol 2012, 180:1928–1941; DOI: 10.1016/j.ajpath.2012.01.020)***

Pancreatic ductal adenocarcinoma (PDAC) is one of the most aggressive human malignancies, and long-term survivors are few. Although the management and treatment of patients with PDAC have improved in the last few decades, the overall 5-year survival rate remains at <5%, and PDAC is the fourth leading cause of cancer death in Japan and the United States.[1] This poor prognosis is due to the fact that PDAC is often locally invasive and is associated with metastases at presentation, which means that the cancer is not resectable. Moreover, those patients who undergo resection frequently exhibit a high incidence of local recurrence, lymph node and hepatic metastasis, and peritoneal dissemination. At the molecular level, the cancer cells in PDAC often harbor mutations in the *KRAS* oncogene and the *SMAD4*, *TP53*, and *CDKN2A* (alias $p16^{Ink4A}$) tumor suppressor genes.[2,3] A high percentage of PDACs also overexpress a number of growth factors and their receptors, including the epidermal growth factor receptor (EGFR), transforming growth factor-α (TGF-α), Cripto-1 growth factor (CRGF), all three TGF-β isoforms, fibroblast growth factor 1 (FGF-1), FGF-2, FGF-5, FGF-7 (also known as keratinocyte growth factor, KGF), and KGFR/FGFR-2 IIIb.[4,5] The concomitant expression of KGF and its receptor in PDAC has been correlated with increased VEGF-A expression, venous invasion, and poor prognosis.[5] These multiple alterations in oncogenes and tumor suppressor genes in conjunc-

Supported by the Japan Society for the Promotion of Science with a Grant-in-Aid for Scientific Research (22591531 to T. I.), Grants-in-Aid for Young Scientists (22689038 to Y.M. and 22790675 to T.Y.), and, in part, by the NIH (R37-CA-075059 to M.K.).

Accepted for publication January 5, 2012.

Supplemental material for this article can be found at *http://ajp.amjpathol.org* or at doi: 10.1016/j.ajpath.2012.01.020.

Address reprint requests to Toshiyuki Ishiwata, M.D., Ph.D., Departments of Pathology and Integrative Oncological Pathology, Nippon Medical School, 1-1-5 Sendagi, Bunkyo-ku, Tokyo, 113-8602, Japan. E-mail: ishiwata@nms.ac.jp.

tion with the overexpression of mitogenic and angiogenic growth factors and their receptors that activate aberrant autocrine and paracrine pathways combine to contribute to the biological aggressiveness of PDAC.

The FGF family consists of FGF-1, FGF-2, FGF-3 (proto-oncogene Int-2), FGF-4 (HST/K-FGF), FGF-5, FGF-6, FGF-7, FGF-8 [androgen-induced growth factor (AIGF)], glia activating factor (GAF) (FGF-9), FGF-10, FGF-11 [FGF homologous factor 3 (FHF-3)], FGF-12 (FHF-1), FGF-13 (FHF-2), FGF-14 (FHF-4), and FGF-16 to FGF-23.[5,6] The FGFs bind to four distinct high-affinity FGF receptors (FGFR-1 to FGFR-4) and to low-affinity heparan sulfate proteoglycans that enhance ligand presentation to the high-affinity receptors.[7] FGFRs are single transmembrane receptors containing extracellular, transmembrane, and intracellular domains. The extracellular domain of FGFRs is usually composed of three Ig-like domains (I to III), and the alternative splicing of C-terminal half of the third Ig-like domain generates IIIb and IIIc isoforms in FGFR-1, FGFR-2, and FGFR-3. Expression of the FGFR-1 IIIb isoform in pancreatic cancer cells inhibits the proliferation, migration, and invasion of these cells, whereas expression of the FGFR-1 IIIc isoform promotes mitogenic signaling via the FRS2-MAPK pathways.[8–11]

In normal human tissues, FGFR-2 IIIb is mainly localized in epithelial cells, whereas FGFR-2 IIIc is mostly expressed in mesenchymal cells.[12] Appropriate tissue-specific expression of FGFR-2 IIIb or FGFR-2 IIIc, in conjunction with the presence of appropriate ligands, is crucial for maintenance of cellular homeostasis and function. FGFs 1, 3, 7, 10, and 22 are reported to bind to FGFR-2 IIIb with high affinity, whereas FGFs 1, 2, 4, 6, 9, 17, and 18 bind to FGFR-2 IIIc with high affinity.[13,14] Previously, FGFs 1, 2, 5, and 7 were reported to be overexpressed in PDAC.[15–17] A significant positive correlation has been demonstrated between FGF-7 and/or FGFR-2 IIIb expression and venous invasion, increased VEGF-A expression, and poor prognosis in PDAC patients.[5] FGFR-2 IIIc expression has been reported in prostate cancer, ovarian cancer, oral squamous cell carcinoma, breast cancer, bladder cancer, and non-small-cell lung cancer cells.[18–23] Moreover, in rat prostate tumors loss of FGFR-2 IIIb expression and gain of FGFR-2 IIIc expression was associated with tumor progression from androgen dependence to androgen independence,[24] whereas in rat bladder cancer cells FGFR-2 IIIc expression has been correlated with epithelial-to-mesenchymal transition, a process associated with tumor progression and invasion.[25] The relevance of FGFR-2 IIIc to human cancers is underscored by the presence of FGFR-2 IIIc in breast cancer cells in women with more advanced stages of the disease.[26]

Certain growth factors, including epidermal growth factor (EGF) and FGF-2, promote formation of spheres that contain cells with the potential for self-renewal, a well-known feature of cancer stem cells (CSCs). These cells promote cancer aggressiveness by enhancing proliferation, invasion, metastasis, and chemoresistance. Thus, CSCs are currently viewed as potentially important therapeutic targets in several malignancies. Given the observation that FGFR-2 IIIc is associated with aggressive cancer growth, we deemed it important to assess the role of FGFR-2 IIIc in PDAC and to determine whether it may contribute to a CSC niche. Accordingly, we examined the expression and biological actions of FGFR-2 IIIc in pancreatic cancer cell lines and human cancer tissues. We now report that FGFR-2 IIIc is expressed in pancreatic cancer cell lines and in PDAC tissues, and that FGFR-2 IIIc promotes the proliferation and migration of PDAC cells, and confers onto these cells CSC-like features.

Materials and Methods

Materials

Materials were purchased as follows: Immobilon P transfer membrane from Millipore (Yonezawa, Japan); FuGene HD transfection reagent from Roche Diagnostics (Mannheim, Germany); FastPure RNA kit from Takara Bio (Tokyo, Japan); high-capacity cDNA reverse transcription kit, TaqMan gene expression assays for FGFR-3 IIIb (Hs01005396_s1), FGFR-3 IIIc (Hs00997397_s1), FGFR4 (Hs01106908_s1), and 18S rRNA (Hs99999901_s1), Silencer Select custom-designed siRNA (s275290 and s275291), and Silencer negative control siRNA from Applied Biosystems (ABI; Life Technologies, Foster City, CA); *Trans*IT-siQUEST transfection reagent from Mirus Bio (Madison, WI); M-PER mammalian protein extraction reagent and SuperSignal West Dura chemiluminescent substrates from Thermo Fisher Scientific (Rockford, IL); G418 (Geneticin; Gibco BRL, Grand Island, NY); Histofine simple stain MAX PO (R) kits, Histofine simple stain MAX PO (M) kits, and peroxidase-conjugated streptavidin from Nichirei (Tokyo, Japan); biotinylated anti-guinea pig IgG from Vector Laboratories (Burlingame, CA); HRP-conjugated goat anti-rabbit IgG secondary antibodies from American Qualex (San Clemente, CA); human serum from Lonza (Walkersville, MD); Zenon rabbit IgG labeling kit (Z-25351), Hoechst 33342 dye, and Click-iT EdU Pacific Blue flow cytometry assay kit from Invitrogen (Life Technologies, Carlsbad, CA); rabbit IgG (ab37415) from Abcam (Cambridge, UK); 35-μm filter, 8-μm pore size cell culture insert, and BioCoat Matrigel invasion chamber from BD Bioscience (Franklin Lakes, NJ); guinea pig polyclonal anti-swine insulin antibody, rabbit polyclonal anti-human IgG antibody, and mouse monoclonal anti-Ki-67 antibody from Dako (Santa Barbara, CA); rabbit polyclonal anti-extracellular signal-regulated kinase (ERK) 1 antibody (K-23) from Santa Cruz Biotechnology (Santa Cruz, CA); mouse monoclonal anti-human CD31 antibody from AbD Serotec (Kidlington, UK); phospho-p44/42 MAPK (p-ERK) rabbit monoclonal antibody from Cell Signaling Technology (Danvers, MA); recombinant human basic fibroblast growth factor (bFGF, FGF-2) from ReproCELL (Kanagawa, Japan); recombinant human EGF from Austral Biologicals (San Ramon, CA); ultra-low attachment surface plate from Corning (Lowell, MA); recombinant human FGF-7 from R&D Systems (Minneapolis, MN); WST-8 cell counting kit from Wako Pure Chemical Industries (Osaka, Japan); New Sil-

ane II slide glass and malinol mounting medium from Mutoh Chemical (Tokyo, Japan). All other chemicals and reagents were purchased from Sigma-Aldrich (St. Louis, MO).

Pancreatic Cancer Cell Lines

KLM-1, PANC-1, MIAPaCa-2, PK-1, and PK-8 PDAC cell lines were obtained from the Cell Resource Center for Biomedical Research, Institute of Development, Aging and Cancer, Tohoku University (Sendai, Japan); the Capan-1 pancreatic adenocarcinoma cell line was purchased from American Type Culture Collection. The cells were grown in the RPMI 1640 medium containing 10% fetal bovine serum (FBS) at 37°C under a humidified 5% CO_2 atmosphere. Capan-1 cells were incubated under the same conditions in RPMI 1640 medium with 15% FBS.

Patients and Tissues

Tissues from 117 patients with invasive PDAC were obtained for this study. These patients received treatment at Nippon Medical School Hospital (Tokyo, Japan) from 1995 to 2011. None of the patients received preoperative chemotherapy and radiotherapy. The patients were 66 men and 51 women; the median age was 66.9 years (range, 35 to 87 years). Clinicopathologic stage was determined according to the TNM classification system of the International Union Against Cancer (UICC) and was additionally characterized under the Japan Pancreas Society classification (Table 1). Fifty-nine patients were monitored after surgery; the median follow-up period was 15.6 months; 28 patients did not receive any postoperative chemotherapy and 31 patients received adjuvant chemotherapy after surgery. Of those receiving chemotherapy, 13 patients received tegafur-uracil and 12 patients received gemcitabine; 6 patients received tegafur-uracil and gemcitabine. Paraffin-embedded specimens were prepared for immunohistochemical analysis, as described previously.[27] This study was conducted in accordance with the principles embodied in the Declaration of Helsinki, 2008, and informed consent for the use of pancreatic tissues was obtained from each patient. Normal pancreatic tissues were obtained from Human Digestive Tissue Sets and Human Tissue Microarray 1 (both obtained from Novagen, Darmstadt, Germany).

Table 1. Clinicopathologic Features and FGFR2 IIIc Expression in Pancreatic Cancers

	FGFR2 IIIc		
	Positive (>30%)	Negative (≤30%)	*P* value
Sample size	*n* = 84	*n* = 33	
Sex			
F	40	11	NS
M	44	22	
Age, years (mean ± SD = 66.94 ± 0.99)			
<66	40	15	NS
≥67	44	18	
UICC classification			
T (primary tumor)			
T1	3	2	NS
T2	2	1	
T3	37	5	
T4	42	25	
N (regional lymph nodes)			
N0	32	10	NS
N1	52	23	
M (distant metastasis)			
M0	83	33	NS
M1	1	0	
G (histological grading)			
G1	37	10	NS
G2	36	14	
G3	8	8	
G4	3	1	
UICC stage			NS
I	7	4	
II	73	26	
III	4	3	

None of the correlations were significant ($P > 0.05$).
F, female; M, male; NS, not significant; UICC, International Union Against Cancer.

Quantitative Real-Time PCR of FGFR-2 IIIc in Pancreatic Cancer Cells

All pancreatic cancer cells were grown in RPMI 1640 medium supplemented with 10% or 15% FBS for 48 hours. Total RNA extraction was performed using a FastPure RNA kit. Next, cDNA synthesis was performed using a high-capacity cDNA reverse transcription kit according to the manufacturer's protocol. Quantitative real-time PCR (q-PCR) was performed using an ABI StepOnePlus system (Life Technologies). The real-time PCR primers used for FGFR-2 IIIc were nt1693-1716 (5′-GGATATCCTTTCACTCTGCATGGT-3′) and nt1770-1794 (5′-TGGAGTAAATGGCTATCTCCAGGTA-3′) of human FGFR-2 IIIc cDNA (102 bp; accession no. NM_000141.4). As TaqMan probes, 5′-CAGTTCTGCCAGCGCCTGGAAGA-3′ was used for FGFR-2 IIIc. PCR primers used for FGFR-1 IIIb were nt1991-2010 (5′-ACCAGTCTGCGTGGCTCACT-3′) and nt2036-2052 (5′-TGCCGGCCTCTCTTCCA-3′) of human FGFR-1 IIIb cDNA (62 bp; accession no. FJ809917.1). As TaqMan probes, 5′-CACCAGACCTGTGGCAA-3′ was used for FGFR-1 IIIb. PCR primers used for FGFR-1 IIIc were nt1295-1316 (5′-GGACTCTCCCATCACTCTGCAT-3′) and nt1381-1403 (5′-CCCCTGTGCAATAGATGATGATC-3′) of the human FGFR-1 IIIc cDNA (109 bp; accession no. M34186.1). As TaqMan probes, 5′-ACCGTTCTGGAAGCC-3′ was used for FGFR-1 IIIc. The PCR reaction mixture containing 2 μL of template cDNA, 10 μL of TaqMan fast universal PCR master mix and 1 μL of each of TaqMan gene expression assay was placed in a 96-well reaction plate. 18S rRNA, as the internal positive control, was amplified using a TaqMan gene expression assay. The optimized program involved denaturation at 95°C for 20 seconds, followed by 50 cycles of amplification (at 95°C for 1 second and at 60°C for 20 seconds) for FGFR-2 IIIc and 18S rRNA. Results were expressed as target/18S rRNA, as an internal standard concentration ratio. Gene expression measurements were performed in triplicate.

Rabbit Polyclonal Anti-Human FGFR-2 IIIc Antibody

To confirm the expression of FGFR-2 IIIc at the protein level in pancreatic cancer, specific antibody against human FGFR-2 IIIc was prepared, as described previously.[28] The anti-FGFR-2 IIIc antibody used was an affinity-purified rabbit polyclonal antibody raised against a peptide corresponding to amino acids AAGVNTTDKEIEVLYIR of the human FGFR-2 IIIc protein (accession no. NM_000141.4). This sequence is located at the carboxyl-terminal half of the Ig loop closest to the transmembrane region and is specific for FGFR-2 IIIc.

Western Blot Analysis of FGFR-2 IIIc in Pancreatic Cancer Cells

Protein extraction was performed according to the protocol involving the use of M-PER mammalian protein extraction reagent. Briefly, cultured pancreatic cancer cells were solubilized in M-PER reagent with protease inhibitor cocktail for mammalian tissues. Lysates were centrifuged for 10 minutes at 10,000 $\times$ *g* to pellet cell debris. The supernatants were collected and protein concentration was measured by the Bradford method. The cleared protein lysates were subjected to SDS-PAGE under reducing conditions, and the separated proteins were transferred to Immobilon P transfer membranes, which were then incubated for 16 hours at 4°C with the anti-FGFR-2 IIIc antibody. The membranes were washed and incubated with HRP-conjugated anti-rabbit IgG antibody for 60 minutes. After the wash, the blot was visualized by enhanced chemiluminescence. The membrane was reblotted with mouse monoclonal anti-β-actin antibody to confirm equal loading.

Immunohistochemistry

The same anti-FGFR-2 IIIc antibody used for Western blotting was also used for immunohistochemistry. Paraffin-embedded sections (3 μm thick) were subjected to immunostaining using a Histofine simple stain MAX PO (R) kit for FGFR-2 IIIc or a Histofine simple stain MAX PO (M) kit for Ki-67 and CD31. After deparaffinization, endogenous peroxidase activity was blocked by incubation for 30 minutes with 0.3% hydrogen peroxide in methanol for FGFR-2 IIIc and Ki-67 antibodies. The tissue sections were then incubated with the anti-FGFR-2 IIIc antibody (1:200 dilution), anti-Ki-67 antibody (1:100 dilution), or CD31 (1:50 in dilution) in phosphate-buffered saline (PBS) containing 1% bovine serum albumin (BSA) for 16 hours at 4°C. Bound antibodies were detected with the Histofine simple stain MAX PO (R) or (M) reagent, using diaminobenzidine tetrahydrochloride as the substrate. For insulin staining, guinea pig polyclonal anti-porcine insulin antibodies (1:1000 dilution), cross-reactive with human insulin, and a biotinylated goat anti-guinea pig IgG secondary antibody were used after incubation with 10% normal goat serum. Sections were then treated with streptavidin-peroxidase complex, using diaminobenzidine tetrahydrochloride as the substrate. The sections were then counterstained with Mayer's hematoxylin. Negative control tissue sections were prepared by omitting the primary antibody.

In Situ *Hybridization*

In situ hybridization was performed as previously reported.[5,29] Tissue sections were deparaffinized and incubated at room temperature for 20 minutes with 0.2 mol/L HCl and then at 37°C for 15 minutes with 100 μg/mL proteinase K. The sections were then postfixed for 5 minutes in PBS containing 4% paraformaldehyde, and incubated twice for 15 minutes each with PBS containing 2 mg/mL glycine at room temperature and once in 50% (v/v) formamide/2$\times$ standard saline citrate for 1 hour at 42°C before initiation of the hybridization reaction. The hybridization buffer contained 0.6 mol/L NaCl, 1 mmol/L EDTA, 10 mmol/L Tris-HCl (pH 7.6), 0.25% SDS, 200 mg/mL yeast tRNA, l$\times$ Denhardt's solution, 10% dextran sulfate, 40% formamide, and 500 ng/mL of the indicated digoxigenin-labeled riboprobe. Hybridization was performed in a moist chamber for 16 hours at 42°C. The sections were then washed sequentially with 2$\times$ standard saline citrate for 20 minutes at 42°C and 0.2$\times$ standard saline citrate for 20 minutes at 42°C. For immunological detection, a DIG nucleic acid detection kit (Roche Diagnostics) was used. The sections were washed briefly with buffer 1 (100 mmol/L Tris-HCl and 150 mmol/L NaCl, pH 7.5), incubated with 1% (w/v) blocking reagents in buffer 1 solution for 60 minutes at room temperature, and with alkaline-phosphatase-conjugated polyclonal sheep anti-digoxigenin Fab fragment containing 0.2% Tween 20 at l:2000 dilution for 60 minutes at room temperature. The sections were then washed twice for 15 minutes at room temperature with buffer 1 solution containing 0.2% Tween 20, equilibrated with buffer 3 solution (100 mmol/L Tris-HCl, 100 mmol/L NaCl, 50 mmol/L $MgCl_2$, pH 9.5) for 2 minutes, and incubated with a staining solution containing nitro blue tetrazolium and X-phosphate in a dark box for 1 hour. After the reaction was stopped with TE buffer (10 mmol/L Tris-HCl and 1 mmol/L EDTA, pH 8.0), the sections were mounted in an aqueous mounting medium.

Construction of FGFR-2 IIIc Expression Vector and Generation of Stably Transfected Clones

The full-length FGFR-2 IIIc cDNA fragment was ligated to the 3′ end of the human cytomegalovirus early promoter/enhancer in pIRES2-EGFP eukaryotic expression vector. Proper orientation of the insert was verified by DNA sequencing. Approximately 1 $\times$ 10^5 cells/2 mL of KLM-1 cells were transfected with 3 μg of DNA using FuGene HD transfection reagent, and the cells were passaged and cultured with 600 μg/mL of G418. Independent colonies were isolated by ring cloning, transferred to microtiter wells, and expanded in 300 μg/mL of G418.

Flow Cytometry of FGFR-2 IIIc

Anti-FGFR-2 IIIc antibody was labeled with allophycocyanin using a Zenon rabbit IgG labeling kit according to the manufacturer's protocol. Cells were incubated for 20 minutes at 4°C in PBS containing 10% human serum. Cells were then centrifuged briefly to remove the serum-containing medium and incubated (5×10^5 cells/25 μL) with 1 μg of allophycocyanin-labeled anti-FGFR-2 IIIc antibody for 60 minutes in the dark at 4°C; 1 μg of propidium iodide was added, to label dead cells. Cells were washed with cold PBS containing 2% FBS, and the cell suspension was passed through a 35-μm filter. FGFR-2 IIIc expression was analyzed using a FACSAria II flow cytometer (BD Bioscience, Franklin Lakes, NJ). Isotype-matched rabbit IgG was used as a negative control.

Morphological Analysis of FGFR-2 IIIc-Transfected KLM-1 Cells

KLM-1 cells were cultured in 75-cm^2 flasks in RPMI 1640 medium containing 10% FBS for 48 hours. The cells were photographed using a Nikon Eclipse TE-2000-U system at ×200 magnification.

Cell Proliferation Assay

To monitor cell proliferation, nonradioactive cell proliferation assays were performed. Cells were plated at a density of 5×10^3 cells per well in 96-well plates and grown overnight in the RPMI 1640 medium supplemented with 10% FBS. After 72 hours, cells were incubated with WST-8 cell counting reagent for 4 hours at 37°C and the optical density of the culture solution in the plate was measured using an enzyme-linked immunosorbent assay (ELISA) plate reader (Bio-Rad Laboratories, Hercules, CA) at 450 nm. Analysis was performed in triplicate.

Heterotopic and Orthotopic Implantation of FGFR-2 IIIc-Transfected KLM-1 Cells

To assess the effect of FGFR-2 IIIc expression on *in vivo* tumorigenicity, 1×10^6 cells/animal were injected subcutaneously into 6-week-old male athymic (nude) mice (BALB/cA Jcl-*nu*/*nu*; CLEA Japan, Tokyo, Japan) ($n = 6$ per cell line). Tumor volume was calculated as $a \times b^2 \times 0.5$, where a is the longest diameter and b is the shortest diameter.[30] The tumors were removed and cut in half. Half of the tumor was fixed in 20% neutral-buffered formalin; the other half, used for orthotopic implantation, was cut into 2-mm^2 pieces. Under brief general inhalation anesthesia with isoflurane and using 7.0 Prolene sutures, KLM-1 fragments (2 mm^2) were sutured onto the surface of the tail of the pancreas of 6-week-old male NOD/Shi-*scid*, IL-2γ^{null} (NOG; Central Institute for Experimental Animals, Kanagawa, Japan) and nude mice ($n = 4$ per cell line).[31] The animals were monitored for 5 weeks.

Sphere Formation Assay

An important feature of stem cells and CSCs (or cancer initiating cells) is formation of cell spheres in floating culture.[32] Therefore, to determine whether pancreatic cancer cells have CSC-like characteristics, we performed sphere formation assays. KLM-1 cells (1000/well) were plated in ultra-low attachment surface 24-well plates with serum-free medium supplemented with or without FGF-2 (10 ng/mL) and EGF (20 ng/mL). After 7 days, the number of spheres in each well was counted under a phase-contrast microscope (Nikon Eclipse TE2000-U). Analysis was performed in triplicate.

Flow Cytometry for Side Population Assay

Cells (1×10^6/mL) were incubated at 37°C for 10 minutes, and then 5 μg/mL of Hoechst 33342 dye was added. Verapamil (30 μg/mL) was also added as a control. Cells were incubated at 37°C for 90 minutes, and then washed twice with cold PBS containing 2% FBS. Cells were suspended with PBS containing 1 mmol/L EDTA, 25 mmol/L HEPES pH 7.0, and 1% FBS. Propidium iodide (1 μg) was added to label dead cells. The cell suspension was passed through a 35-μm filter. The ratio of side population (SP) to major population (MP) was analyzed using a BD FACSAria II flow cytometer. Analysis was performed in triplicate.

Tumorigenicity of SP and MP Cells in KLM-1 Cells

To examine the tumor formation ratio of SP and MP cells in KLM-1 cells, we sorted each cells by flow cytometry, as described above. A total number of 10^5, 10^4, 10^3, or 10^2 cells of SP and MP fractions were subcutaneously injected into 6-week-old male NOD.CB17-*Prkdc*^{scid}/J (NOD/SCID) mice (Charles River Laboratories Japan, Kanagawa, Japan). Tumor formation was determined after 5 weeks.

Cell Cycle Flow Cytometry

Cell cycle analysis was performed using a Click-iT EdU Pacific Blue flow cytometry assay kit according to the manufacturer's protocol. In brief, 10 μmol/L of 5-ethynyl-2′-deoxyuridine (EdU) was added into culture medium, and cells were incubated for 60 minutes at 37°C. Cells were fixed with 4% paraformaldehyde for 60 minutes, and then the EdU was labeled with Pacific Blue. 7-Aminoactinomycin D (7-AAD) was added for measuring DNA content and cell cycle distribution, and cell cycle analysis was performed using a BD FACSAria II flow cytometer.

Cell Signaling Pathway of FGFR-2 IIIc-Transfected Pancreatic Cancer

Cells were seeded in 60 mm-dish (2.5×10^5 cells) and grown in RPMI 1640 medium supplemented with 10% FBS for 24 hours. The cells were then washed with serum-

free medium and cultured with same medium for 24 hours, and recombinant FGF-2 (100 ng/mL) and/or heparin (1 μg/mL) was added to the plates. Protein was then extracted and used for the Western blot analyses using rabbit monoclonal anti-p-ERK (1:1000) and rabbit polyclonal anti-ERK antibodies (1:1000), as described above.

Single-Cell Movement Assay

Cells (5×10^3 per well) were seeded onto a four-well glass-bottom dish and grown for 24 hours, and the medium was then changed to RPMI 1640 supplemented with 10% FBS, 100 ng/mL FGF-2, or 100 ng/mL FGF-7. Cell movement in the presence of an anti-FGFR-2 IIIc antibody or control IgG was then monitored for 24 hours using a digital Nikon Eclipse TE 2000-E motorized inverted microscope, acquiring images every 5 minutes. The total distance that individual cells traveled during 24 hours was determined using MetaMorph software version 7.6 (Universal Imaging, Marlow, UK).

Transfection of FGFR-2 IIIc siRNA

Down-regulation of FGFR-2 IIIc expression in PANC-1 cells was induced using siRNA. Two different types of custom-designed siRNA against specific IIIc region of FGFR-2 IIIc were purchased, and the sense sequence was 5′-GGAAUGUAACUUUUGAGGATT-3′ (s275290) and 5′-GUGCUUGGCGGGUAAUCCUTT-3′ (s275291) (underlining denotes common sequences). The cells were plated at a density of 1×10^5 cells in a 35-mm dish and transfected with 5 nmol/L siRNAs for FGFR-2 IIIc and Silencer negative control siRNA for control using *Trans*IT-siQUEST according to the manufacturer's protocol. To confirm the effective transfection of siRNA in PANC-1 cells, total RNA was prepared at 24 hours after the transfection and FGFR-2 IIIc mRNA levels were determined by q-PCR.

Effects of Anti-FGFR-2 IIIc Antibody on Cell Migration and Invasion

Cell migration was assessed using modified Boyden chambers with uncoated inserts (6.4 mm in diameter; 8-μm pores). Serum-free RPMI 1640 medium (500 μL) was placed in each upper chamber and RPMI 1640 medium with 10% FBS (750 μL) was into placed in each lower chamber. PANC-1 cells were then plated on the inner surface of the inserts at a density of 1×10^5 cells per insert in the presence of either the anti-FGFR-2 IIIc antibody or control IgG (100 μg/mL), followed by incubation at 37°C in a humidified 5% CO_2 atmosphere. After 6 hours, the cells that moved to the outer surface of the inserts were fixed, stained with a Diff-Quik staining kit (Fisher Scientific, Pittsburgh, PA), and counted in five high-power fields (20× objective). All assays were performed in triplicate. Cell invasion assays were performed using modified Boyden chambers in which the inner surfaces of the inserts were coated with Matrigel. Cell counting was performed as described above.

Statistical Analysis

Results for cell proliferation or tumor volume are presented as means ± SE. Data were compared between different groups using Student's *t*-test. Whenever indi-

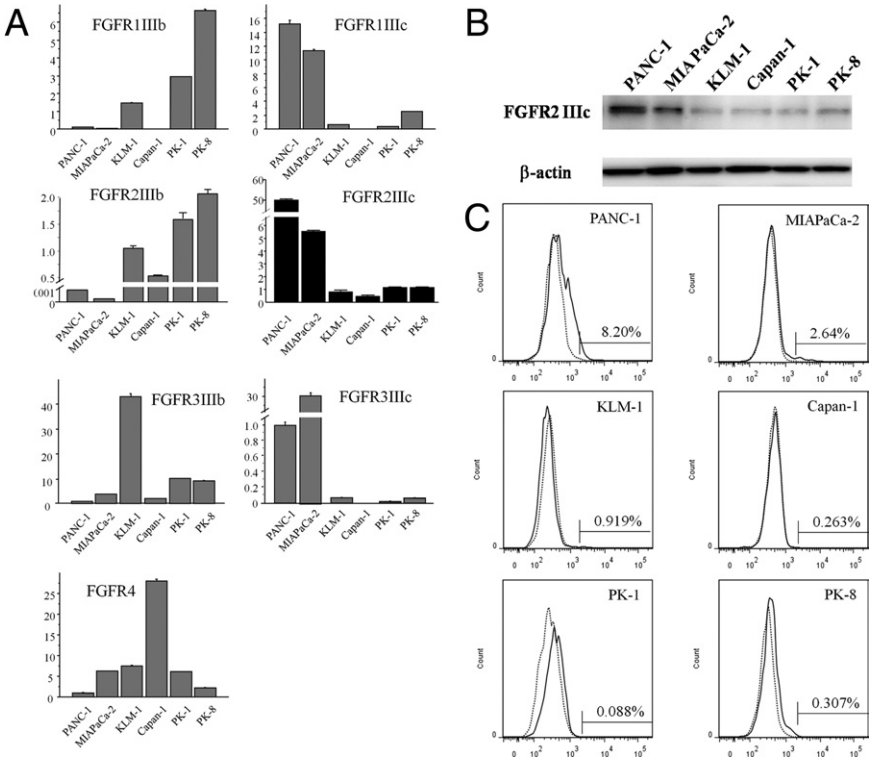

Figure 1. Quantitative real-time PCR, Western blotting, and flow cytometry analysis of FGFR-2 IIIc in pancreatic cancer cell lines. Cells of six pancreatic cancer cell lines were grown in RPMI 1640 medium with 10% or 15% FBS for 48 hours. **A:** FGFR-2 IIIc mRNA and other FGFRs were expressed at variable levels in all six cell lines. FGFR-2 IIIc mRNA levels were highest in PANC-1 cells, which expressed 106-fold higher levels of this mRNA moiety, compared with Capan-1 cells. **B:** A band corresponding to 100-kDa FGFR-2 IIIc protein was detected in all pancreatic cancer cell lines at levels that closely paralleled the corresponding mRNA levels. β-Actin protein levels indicated nearly equal loading of total proteins in all lanes. **C:** FGFR-2 IIIc-overexpressing cells were detected most frequently in the PANC-1 and MIA PaCa-2 cell lines. Isotype-matched rabbit IgG was used as a negative control (**dotted line**).

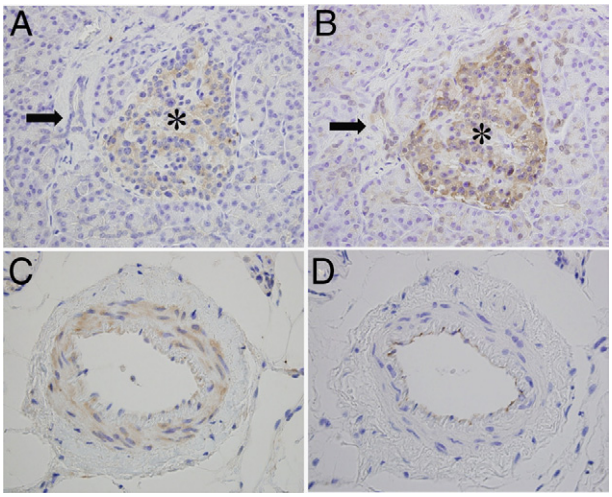

Figure 2. Immunohistochemical analysis of FGFR-2 IIIc in normal pancreatic tissues. Serial tissue sections of normal pancreas stained for FGFR-2 IIIc (**A** and **C**), insulin (**B**), and CD31 (**D**). FGFR-2 IIIc immunoreactivity was weakly detected in the islet cells (**asterisks**), but not in ductal cells (**arrows**), acinar cells, or capillary endothelial cells. FGFR-2 IIIc was localized in the vascular endothelial cells and vascular smooth muscle cells in peripancreatic tissues (**C**). Serial tissue sections indicate that CD31 is expressed in the endothelial cells (**D**). Original magnification, ×400.

cated, the χ^2 test and Fisher's exact test were used to analyze the correlation between FGFR-2 IIIc expression and clinicopathologic features. Cumulative survival rates were calculated by the Kaplan-Meier method, and the significance of differences in survival rate was analyzed by the log-rank test. Data were compared between multiple groups using one-way analysis of variance and then analyzed using a post hoc test. $P < 0.05$ was considered significant in all analyses. Computations were performed using the StatView J version 5.0 software package (SAS Institute, Cary, NC).

Results

FGFR Isoform Expression in Pancreatic Cancer Cell Lines

To determine whether cultured human pancreatic cancer cell lines express FGFR-2 IIIc, and to compare any such expression with the expression of other FGFR isoforms, q-PCR was performed using RNA from six human pancreatic cancer cell lines. FGFR-2 IIIc mRNA was expressed in all six cell lines. FGFR-2 IIIc mRNA levels were highest in PANC-1 cells, intermediate in MIA PaCa-2 cells, and relatively low in KLM-1, Capan-1, PK-1, and PK-8 cells (Figure 1A). The FGFR-2 IIIc level was 106-fold higher in PANC-1 cells than in Capan-1 cells, which demonstrates the extent of variability of FGFR-2 IIIc mRNA levels across the different cell lines. PANC-1 and MIA PaCa-2 cells (which express high levels of FGFR-2 IIIc) expressed low FGFR-2 IIIb, whereas KLM-1, Capan-1, PK-1, and PK-8 cells (which express low FGFR-2 IIIc) expressed higher FGFR-2 IIIb levels. A similar tendency was observed in the expression levels of FGFR-1 and FGFR-3 isoforms in the pancreatic cancer cell lines (Figure 1A).

Next, immunoblotting with an anti-FGFR-2 IIIc antibody was performed, using protein lysates from the same six pancreatic cancer cell lines. FGFR-2 IIIc was expressed

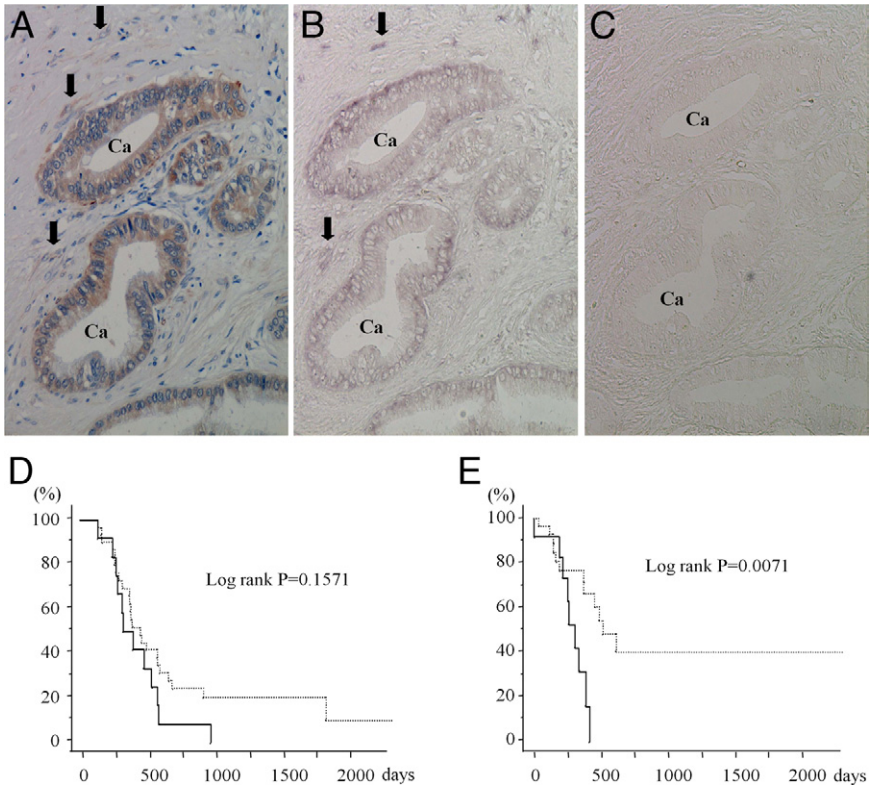

Figure 3. Serial tissue sections of IHC and *in situ* hybridization analyses of FGFR-2 IIIc in human pancreatic cancer tissues. **A–C:** FGFR-2 IIIc and its mRNA were strongly expressed in pancreatic cancer cells (Ca) and fibroblast adjacent to cancer cells (**arrows**). Sense probe did not yield positive signals (**C**). **D:** Overall survival curves showed a tendency to worse prognosis in the FGFR-2 IIIc-positive group (**solid line**) ($P = 0.1571$). **E:** Duration to development of liver metastasis after surgery was significantly shorter in FGFR-2 IIIc-positive groups (**solid line**) than in the FGFR-2 IIIc-negative groups (**dotted line**) ($P = 0.0071$). Original magnification, ×200.

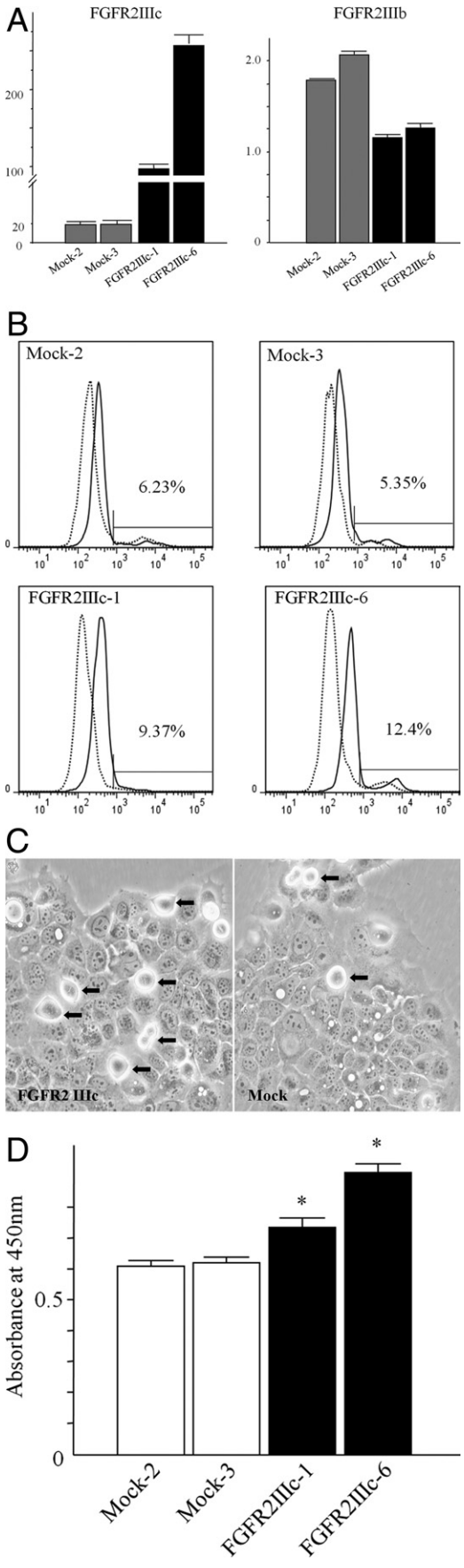

at the protein level in all the cell lines (Figure 1B). FGFR-2 IIIc protein was most abundant in PANC-1 cells and least abundant in KLM-1, Capan-1, PK-1, and PK-8 cells (Figure 1B). Analysis by flow cytometry revealed similar expression patterns for FGFR-2 IIIc at the cell surface of the PDAC cells as determined by Western blotting (Figure 1C). Overall, there was a close correlation between FGFR-2 IIIc mRNA and protein levels in all six pancreatic cancer cell lines.

FGFR-2 IIIc Expression in Pancreatic Cancer Tissues

Immunohistochemical and *in situ* hybridization analysis of PDAC samples was performed next, to determine whether and in which cell type FGFR-2 IIIc is expressed in human pancreatic cancer tissues. In the normal pancreas, weak FGFR-2 IIIc immunoreactivity was detected in the endocrine islets, but not in ductal cells or capillary endothelial cells (Figure 2A), and strong insulin immunoreactivity was present in the islets (Figure 2B). Moderate FGFR-2 IIIc immunoreactivity was evident in the vascular smooth muscle cells and endothelial cells of relatively large vessels in the peripancreatic tissues (Figure 2C). As expected, the vascular endothelial cells were positive for CD31 (Figure 2D). By contrast to the epithelial cells in the normal pancreas, there was strong FGFR-2 IIIc immunoreactivity in the cancer cells in 84 of 117 (71.8%) PDAC samples (Figure 3A and Table 1). Moderate FGFR-2 IIIc immunoreactivity was also evident in the fibroblasts adjacent to cancer cells (Figure 3A). Both the cancer cells and the fibroblasts exhibited a moderately strong FGFR-2 IIIc mRNA in *in situ* hybridization (Figure 3B). A sense probe used as negative control did not yield a signal (Figure 3C).

FGFR-2 IIIc expression in the cancer cells did not correlate with the clinicopathological factors (Table 1). The overall 2-year survival rate for all 59 cases of PDAC was 16.9%, and the overall survival rates of the FGFR-2 IIIc-positive group tended to be lower, but this difference was not statistically significant ($P = 0.1571$) (Figure 3D). Time to development of liver metastasis after resection was significantly shorter in the FGFR-2 IIIc-positive group than in the FGFR-2 IIIc-negative group ($P = 0.0071$) (Figure 3E).

Figure 4. Consequences of FGFR-2 IIIc transfection in KLM-1 cells. **A:** KLM-1 cells were grown in RPMI 1640 medium with 10% FBS for 48 hours, total RNA was extracted, and cDNA synthesis and q-PCR were performed. FGFR-2 IIIc mRNA/18S ribosomal RNA levels were markedly increased in two FGFR-2 IIIc-transfected clones (clones 1 and 6), but not in mock-transfected cells (mock-2 and mock-3). FGFR-2 IIIb mRNA expression was decreased in FGFR-2 IIIc-transfected clones. **B:** Flow cytometry revealed greater numbers of FGFR-2 IIIc-expressing cells on the cell surface in FGFR-2 IIIc-transfected KLM-1 cells, compared with in mock-transfected cells Isotype-matched rabbit IgG was used as a negative control (**dotted line**). **C:** FGFR-2 IIIc-transfected KLM-1 cells and mock-transfected cells were morphologically indistinguishable, except for the presence of a greater number of cells undergoing mitosis in the FGFR-2 IIIc-transfected KLM-1 cells (**arrows**). Original magnification × 200. **D:** When plated at a density of 5×10^3 cells per well in a 96-well plate and grown for 72 hours in the RPMI 1640 medium supplemented with 10% FBS, FGFR-2 IIIc-transfected KLM-1 cells demonstrated a significant increase in proliferation, compared with mock cells. $^*P < 0.05$.

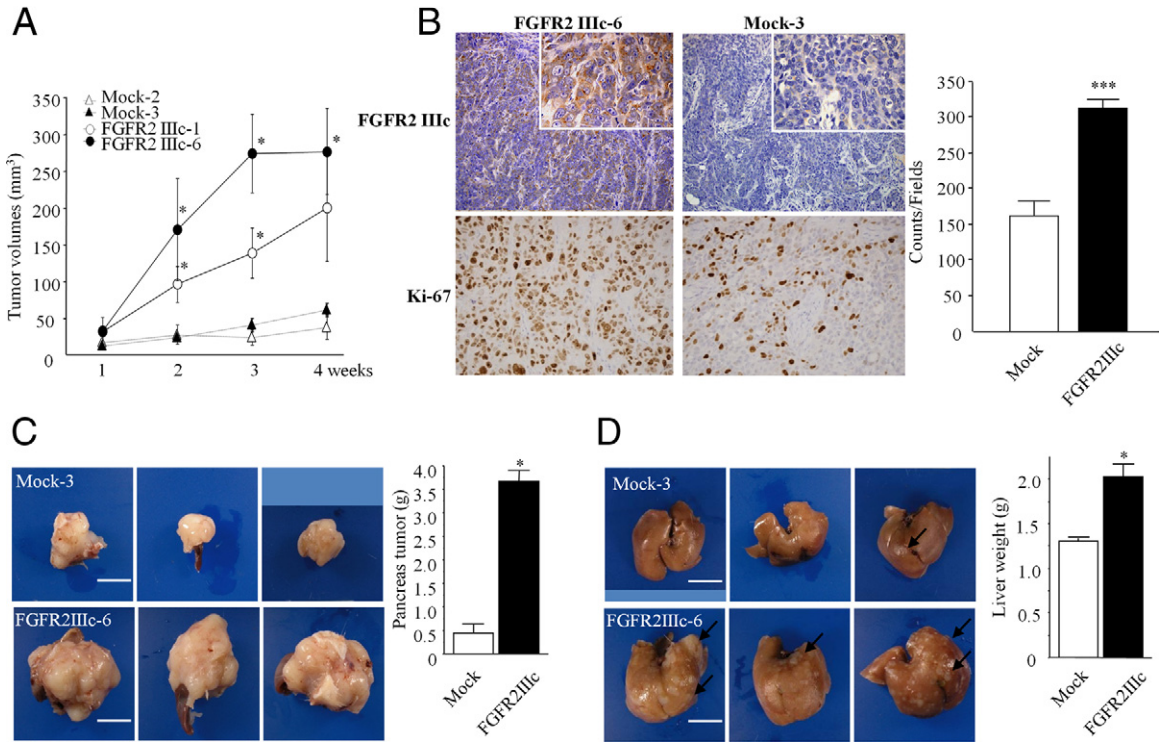

Figure 5. Effects of FGFR-2 IIIc on the proliferation and metastasis of KLM-1 cells in immunodeficient mice. **A:** FGFR-2 IIIc-transfected KLM-1 cells formed larger subcutaneous tumors, compared with mock-transfected cells. **B:** The tumors were removed, and immunohistochemical analysis was performed using anti-FGFR-2 IIIc or anti-Ki-67 antibodies. FGFR-2 IIIc immunoreactivity was more strongly expressed in FGFR-2 IIIc-transfected cells (FGFR-2 IIIc-6), compared with mock-transfected cells (mock-3). The Ki-67 labeling index was higher in tumors arising from FGFR-2 IIIc-transfected KLM-1 cells, compared with mock-transfected cell derived tumors. **C:** In the orthotopic model, FGFR-2 IIIc-transfected-KLM-1 cells formed larger primary tumors, compared with mock-transfected cells. Moreover, pancreatic tumor weights were significantly elevated in FGFR-2 IIIc-transfected cells, compared with mock-transfected cells. **D:** The number of liver metastases was also increased in FGFR-2 IIIc-transfected KLM-1 cells (**arrows**), in conjunction with an increase in liver weight in FGFR-2 IIIc-transfected cells. $^{*}P < 0.05$; $^{***}P < 0.0001$. Original magnification: ×200 (**B**, **top**); ×400 (**B**, **bottom**); ×600 (**B**, **insets**). Scale bar = 10 mm.

Stable FGFR-2 IIIc-Transfected KLM-1 Cells

To examine the role of FGFR-2 IIIc in pancreatic cancer cells, we prepared FGFR-2 IIIc-overexpressing pancreatic cancer cells and mock-transfected cells as controls. A full-length FGFR-2 IIIc cDNA was subcloned into pIRES2-EGFP vector and stably transfected into KLM-1 cells, which express a low level of FGFR-2 IIIc. Capan-1 cells were not suitable for stable transfection, because, although they expressed the lowest level of FGFR-2 IIIc, these cells grow very slowly. FGFR-2 IIIc mRNA levels in mock-transfected cells and FGFR-2 IIIc-transfected KLM-1 cells were examined by q-PCR in relation to the 18S rRNA housekeeping gene. FGFR-2 IIIc/18S rRNA levels were very high in FGFR-2 IIIc clones 1 and 6 and low in the mock clones (Figure 4A). There was a parallel but relatively small decrease in IIIb mRNA levels in the FGFR-2 IIIc-transfected clones (Figure 4A). Moreover, as analyzed with flow cytometry using the anti-FGFR-2 IIIc antibody, high levels of FGFR-2 IIIc protein were evident in FGFR-2 IIIc stably transfected KLM-1 cells (Figure 4B), indicating that FGFR-2 IIIc was abundant on the cell surface of these clones. FGFR-2 IIIc transfection did not alter FGFR-3 IIIb or FGFR4 levels (see Supplemental Figure S1 at *http://ajp.amjpathol.org*), and the levels of the other FGFRs were exceedingly low (data not shown).

Effects of FGFR-2 IIIc on Cell Morphology and Proliferation

FGFR-2 IIIc-transfected KLM-1 cells and the corresponding mock-transfected cells exhibited similar morphologies. However, the number of mitotic cells was greater in the FGFR-2 IIIc-transfected KLM-1 cells than in mock-transfected cells (Figure 4C). Moreover, FGFR-2 IIIc stably transfected KLM-1 cells demonstrated increased cell proliferation, compared with mock cells (Figure 4D).

Effects of FGFR-2 IIIc on Subcutaneous Tumor Formation in Nude Mice

To determine whether FGFR-2 IIIc modulated the *in vivo* proliferation of pancreatic cancer cells, FGFR-2 IIIc-transfected KLM-1 cells and mock-transfected cells were injected subcutaneously in nude mice. Compared with two different mock clones, FGFR-2 IIIc-transfected KLM-1 clones 1 and 6 formed significantly larger tumors (Figure 5A). There was strong FGFR-2 IIIc immunoreactivity in the FGFR-2 IIIc-6-derived tumors and weak immunostaining in the mock-3-derived tumors (Figure 5B). FGFR-2 IIIc immunoreactivity was not detected in stromal cells in the nude mice. Moreover, there was a marked increase in Ki-67 immunoreactivity in the FGFR-2 IIIc-6-derived tumors, com-

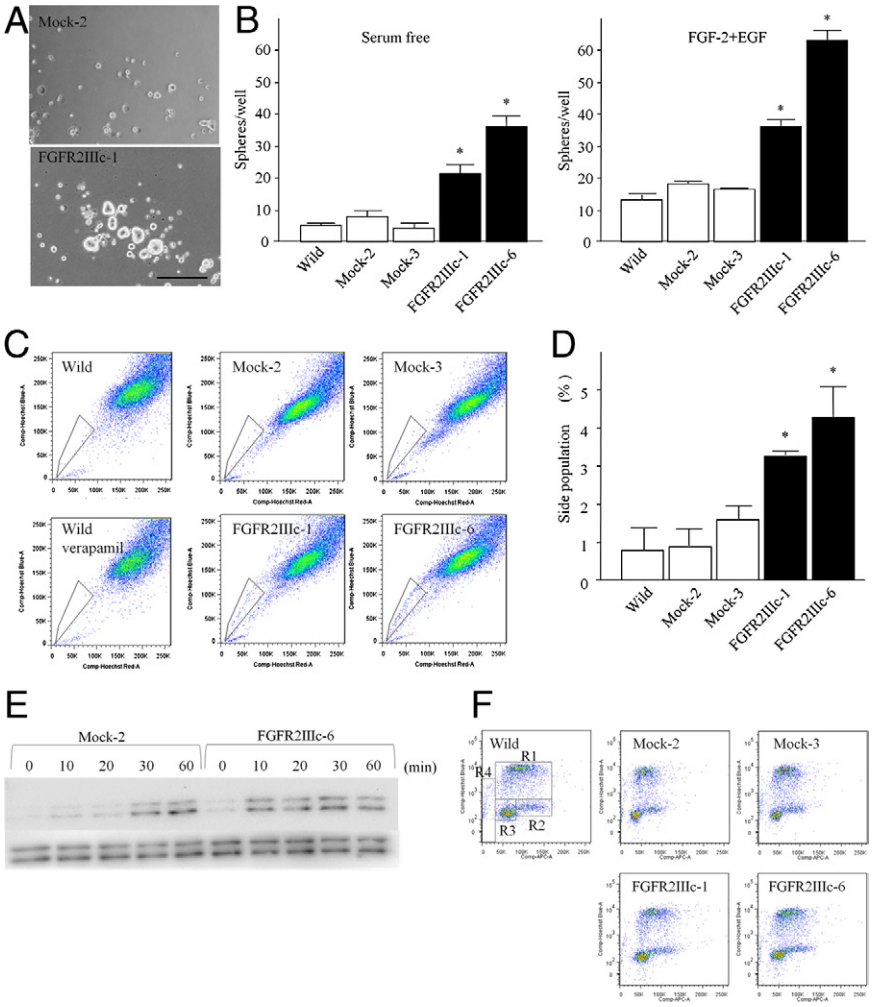

Figure 6. Sphere formation and side population assays in KLM-1 cells. KLM-1 cells were plated on ultra-low attachment surface plates with serum-free medium in the absence or presence of FGF-2 (10 ng/mL) and EGF (20 ng/mL), and cultured for 7 days. **A:** FGFR-2 IIIc-transfected cells formed larger spheres, compared with mock-transfected cells. Original magnification, ×100. Scale bar = 100 μm. **B:** In serum-free medium, FGFR-2 IIIc-transfected KLM-1 formed more spheres, compared with mock and wild cells. Addition of FGF-2 and EGF increased the number of spheres, but FGFR-2 IIIc-transfected KLM-1 cells still formed more spheres, compared with mock or parental cells. **C:** After Hoechst 33342 dye staining, the side population of the cells was measured by flow cytometry. **D:** The proportion of SP cells was increased in FGFR-2 IIIc-transfected KLM-1 cells, compared with mock and wild cells. **E:** FGF-2 (100 ng/mL) increased ERK phosphorylation to a greater extent in FGFR-2 IIIc-transfected KLM-1 cells, compared with mock-transfected cells. Immunoblotting for total ERK confirmed equivalent loading of lanes. **F:** Apoptotic cell numbers were decreased in FGFR-2 IIIc-transfected cells, compared with wild and mock-transfected cells. R1, S phase; R2, G2+M phase; R3, G0/G1 phase; R4, sub-G0/G1. $^*P < 0.05$.

pared with the mock-3-derived tumors, and the calculated Ki-67 labeling index in the subcutaneous tumor was twofold higher in FGFR-2 IIIc-transfected KLM-1 cells, compared with mock-transfected cells (Figure 5B).

Effects of FGFR-2 IIIc on Orthotopic Tumor Formation and Liver Metastasis in NOG Mice

We next performed orthotopic implantation of FGFR-2 IIIc-transfected KLM-1 cells into NOG mice. FGFR-2 IIIc-transfected KLM-1 cells formed larger intrapancreatic tumors, compared with mock-transfected cells, and the tumors were significantly heavier (Figure 5C). In addition, in this model, liver metastases were detected in all four tumors derived from FGFR-2 IIIc-transfected cells, but only in two of the four mock-transfected cell-derived tumors. The number of liver metastases was also increased in FGFR-2 IIIc-transfected cells, compared with mock-transfected cells, and the livers of FGFR-2 IIIc-expressing tumors were significantly heavier (Figure 5D).

Orthotopic implantation was also performed in nude mice, which have greater immunological responses than NOG mice. In this model, the mean intrapancreatic tumor weight of the four FGFR-2 IIIc-6-derived tumors was 0.804 ± 0.275 g. By contrast, the mean weight of the four mock-3-derived tumors was 0.357 ± 0.023 g. Moreover, liver metastases were observed in only one mouse implanted with FGFR-2 IIIc-6 expressing tumor fragments, and in none of the four mice implanted with mock-3 expressing tumor fragments.

Effects of FGFR-2 IIIc on Sphere Formation and Side Population

To determine whether FGFR-2 IIIc contributed to CSC-like features, we performed sphere formation and SP

Table 2. Tumor Formation Ratio 5 Weeks after Subcutaneous Injection of KLM-1 Cells in NOD/SCID Mice

	Tumor Formation Proportion by cells/mouse [% (*n*/*N*)]			
Population	1.0×10^2	1.0×10^3	1.0×10^4	1.0×10^5
MP	0 (0/6)	0 (0/6)	33.3 (2/6)	66.7 (4/6)
SP	0 (0/6)	0 (0/6)	66.7 (4/6)	100 (6/6)

MP, major population cells; SP, side population cells.

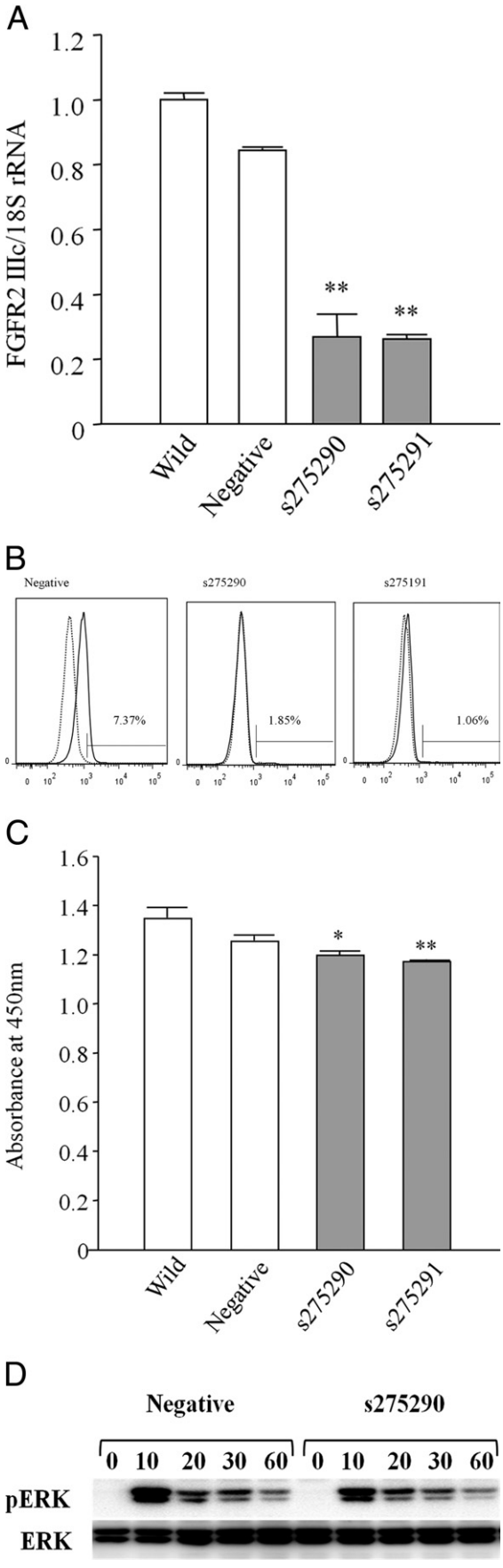

assays in FGFR-2 IIIc-overexpressing pancreatic cancer cells. In the sphere formation assay, FGFR-2 IIIc-transfected cells formed larger (Figure 6A) and more numerous (Figure 6B) spheres, compared with mock-transfected cells. Next, the proportion of SP fraction in pancreatic cancer cells was determined by flow cytometry (Figure 6C). FGFR-2 IIIc-transfected cells (FGFR-2 IIIc-1 and -6) also exhibited increased SP fractions, compared with mock and wild (parental) cells (Figure 6D). Subcutaneous injection of SP and MP cells of KLM-1 cells into NOD/SCID mice, revealed that the tumors formed when either 1.0×10^4 or 1.0×10^5 cells were injected, but not when fewer cells were injected (Table 2). Moreover, the tumor formation ratio was always higher in SP cells than in MP cells (Table 2).

Mitogenic signaling through FGFRs often involves activation of the MAPK pathway. We therefore sought to determine whether FGF-2-mediated activation of MAPK was altered as a consequence of changes in the levels of FGFR-2 IIIc. FGF-2 caused a rapid increase in p-ERK levels in both mock-2 cells and FGFR-2 IIIc-6 transfected PANC-1 cells. However, the phosphorylation levels of ERK were markedly higher at 10 and 20 minutes after FGF-2 addition in FGFR-2 IIIc-transfected KLM-1 cells (Figure 6E). By contrast, the number of apoptotic cells (sub G0/G1 phase) was decreased in FGFR-2 IIIc-transfected cells (2.12% and 2.80%), compared with wild (4.24%) and mock-transfected cells (3.57% and 4.25%) (Figure 6F).

Transient Transfection of FGFR-2 IIIc in Capan-1 Cells

To confirm our findings with KLM-1 cells, we next assessed the consequences of transient transfection of FGFR-2 IIIc in Capan-1 cells, because these cells exhibited the lowest expression levels of FGFR-2 IIIc mRNA. FGFR-2 IIIc mRNA (see Supplemental Figure S2A at *http://ajp.amjpathol.org*) and protein levels (see Supplemental Figure S2B at *http://ajp.amjpathol.org*) were markedly increased 72 hours after transfection. FGFR-2 IIIc-transfected Capan-1 cells exhibited increased cell proliferation, compared with wild and mock-transfected cells (see Supplemental Figure S2C at *http://ajp.amjpathol.org*). Moreover, FGF-2 and FGF-7 enhanced the migration of Capan-1 cells, but this effect was statistically greater in FGFR-2 IIIc-transfected cells, compared with mock-transfected cells (see Supplemental Figure S2D at *http://ajp.amjpathol.org*).

Figure 7. Effects of FGFR-2 IIIc down-regulation on PANC-1 cell proliferation. FGFR-2 IIIc expression in PANC-1 cells was down-regulated using siRNA against FGFR-2 IIIc transcripts. **A:** Two different siRNA sequences against FGFR-2 IIIc mRNA (s275290 and s275291) down-regulated FGFR-2 IIIc expression at 24 hours after transfection. **B:** The percentage of FGFR-2 IIIc expressing cells was markedly decreased after transfection with FGFR-2 IIIc siRNA, compared with negative siRNA-transfected cells. Isotype-matched rabbit IgG was used as negative control (**dotted line**). **C:** The proliferation rates of these cells were lower than those in control siRNA-transfected cells. **D:** After the addition of FGF-2, FGFR-2 IIIc siRNA-transfected cells (s275290) showed decreased phosphorylation of ERK, compared with negative siRNA-transfected cells. $^*P < 0.05$; $^{**}P < 0.01$.

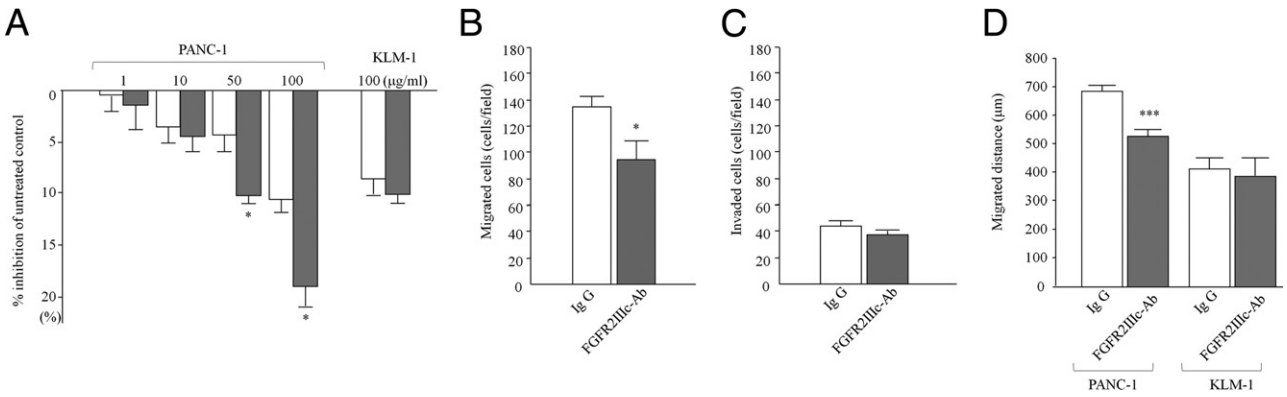

Figure 8. Effects of an anti-human FGFR-2 IIIc antibody on PANC-1 cells. The PANC-1 cells (5×10^3 cells/100 μL) were grown overnight in RPMI 1640 medium supplemented with 10% FBS and then incubated for 48 hours in the absence (open bars) or presence (shaded bars) of the anti-FGFR-2 IIIc antibody at four different concentrations. **A:** Significant inhibition of proliferation was observed at concentrations of 50 and 100 μg/mL of the anti-FGFR-2 IIIc antibody, compared with proliferation rates in the presence of the same concentrations of rabbit IgG. Within 6 hours after its addition, the anti-FGFR-2 IIIc antibody also inhibited the migration of PANC-1 cells (**B**), but did not alter their invasion (**C**). **D:** Inhibition of cell motility was also observed at 24 hours after addition of the anti-FGFR-2 IIIc antibody. In KLM-1 cells, which express very low levels of FGFR-2 IIIc, proliferation and migration were not altered by the addition of FGFR-2 IIIc antibodies. $^*P < 0.05$; $^{***}P < 0.0001$.

Effects of FGFR-2 IIIc Down-Regulation on PANC-1 Cells

To further assess the importance of FGFR-2 IIIc in the modulation of pancreatic cancer cell function, we next sought to examine the consequences of down-regulating FGFR-2 IIIc in PANC-1 cells, which expressed the highest levels of FGFR-2 IIIc among all our cell lines. Accordingly, two different sequences of siRNA against FGFR-2 IIIc mRNA (s275290 and s275291) were used to induce the down-regulation of FGFR-2 IIIc. Both siRNAs markedly decreased FGFR-2 IIIc mRNA levels, compared with those in control siRNA-transfected PANC-1 cells, at 24 hours after transfection (Figure 7A). By flow cytometry, there were fewer FGFR-2 IIIc-expressing cells after transfection with FGFR-2 IIIc siRNA (1.85% and 1.06%), compared with cells transfected with negative siRNA (7.37%) (Figure 7B). Basal proliferation rates of PANC-1 cells transfected with either FGFR-2 IIIc siRNAs were significantly lower than proliferation in control siRNA-transfected cells (Figure 7C). Compared with negative siRNA-transfected cells, FGFR-2 IIIc siRNA-transfected PANC-1 cells showed decreased ERK phosphorylation in response to FGF-2 (Figure 7D).

Next, we sought to determine whether the anti-FGFR-2 IIIc antibody would inhibit the proliferation, migration, and invasion of PANC-1 cells. Incubation of PANC-1 cells with the anti-FGFR-2 IIIc antibody exerted a dose-dependent inhibitory effect on the PANC-1 cell proliferation, maximal inhibition occurring at a concentration of 100 μg/mL, whereas the control rabbit IgG was without effect (Figure 8A). The anti-FGFR-2 IIIc antibody also inhibited the migration of PANC-1 cells (Figure 8B), but did not alter their invasion (Figure 8C). Time-lapse analysis indicated that the anti-FGFR-2 IIIc antibody markedly inhibited cell motility, compared with control IgG (Figure 8D). Proliferation and migration of KLM-1 cells, which express very low levels of FGFR-2 IIIc, were not inhibited by the addition of FGFR-2 IIIc antibodies (Figure 8, A and D).

Discussion

FGFR 2 IIIc and FGFR-2 IIIb/KGFR differ from each other in the carboxyl-terminal half of the Ig-like region closest to the intracellular domain, as a consequence of alternative splicing.[12] FGFR-2 IIIc is widely expressed in various types of cancer cells, including adenocarcinomas, squamous cell carcinomas, and transitional cell carcinomas.[18–24] Most often, FGFR-2 expression correlates with aggressive growth of the cancers and/or acquisition of features consistent with epithelial-to-mesenchymal transition. In the present study, we determined that FGFR-2 IIIc mRNA was expressed in six pancreatic cancer cell lines, and that the levels of the 100-kDa FGFR-2 IIIc protein, as determined by immunoblotting with our highly specific anti-FGFR-2 IIIc antibody, paralleled the corresponding mRNA levels. To our knowledge, this is the first report to document FGFR-2 IIIc expression at the protein level in pancreatic cancer cells.

Using the same antibody, we documented that FGFR-2 IIIc was expressed in 73% of PDAC cases, which represents a higher frequency than the 41.5% frequency of expression previously reported for FGFR-2 IIIb/KGFR.[5] Although the presence of FGFR-2 IIIc correlated with decreased duration to development of liver metastasis after surgery, there was no significant correlation between FGFR-2 IIIc expression and prognosis. Previously, we reported that FGFR-2 IIIb expression correlated with an increased frequency of venous invasion but was not associated with decreased survival. Thus, although the presence of either of these two FGFR-2 isoforms in PDAC is deleterious to the patient, other alterations dictate duration of patient survival.[5] Nonetheless, several distinct lines of evidence suggest that FGFR-2 IIIc contributes to the proliferation and migration of pancreatic cancer cells, which may then secondarily promote retroperitoneal invasion. First, FGFR-2 IIIc stably transfected KLM-1 cells exhibited more rapid proliferation *in vitro* and *in vivo* than mock-transfected cells. Second, transient transfection in PANC-1 cells with two different sequences of FGFR-2 IIIc

siRNA markedly inhibited cell proliferation. Third, a highly specific anti-FGFR-2 IIIc antibody inhibited cell proliferation in a dose-dependent manner. Nonetheless, it is also possible that increased FGFR-2 IIIc expression in the stromal fibroblasts may contribute to formation of chronic pancreatitis-like lesions in PDAC through enhanced proliferation and migration of cancer-associated fibroblasts.

Two mechanisms may explain why increased expression of FGFR-2 IIIc induces pancreatic cancer cell proliferation. First, multiple ligands bind with high affinity to FGFR-2 IIIc, most notably FGFs 1, 2, 4, 6, 9, 17, and 18,[13,14] and several of these ligands are overexpressed in PDAC.[15,33] Second, FGFR-2 IIIc receptor overexpression was associated with more pronounced MAPK phosphorylation, which is known to activate mitogenic signaling. Although the changes in proliferation induced by attenuating FGFR-2 IIIc expression in PANC-1 cells were relatively modest, they were statistically significant. Moreover, it has been recently demonstrated that cancer cell proliferation is only slightly increased *in vivo*, compared with proliferation rates in normal cells, and that the cumulative effects of this slight increase in proliferation lead after many years to enhanced tumor size and, ultimately, to gene alterations that lead to metastasis formation.[34] Taken together, these observations suggest that patients whose cancers express high levels of FGFR-2 IIIc may have slightly more rapid disease progression.

In PDAC cell lines, FGFR-2 IIIc and IIIb levels tended to be inversely related. Thus cell lines with high FGFR-2 IIIc levels, such as PANC-1 and MIAPaCa-2 cells, had relatively low levels of FGFR-2 IIIb and cell lines with high FGFR-2 IIIb levels, such as PK-1 and PK-8 cells, had relatively low levels of FGFR-2 IIIc. These observations are consistent with recent studies showing that epithelial splicing regulatory proteins 1 and 2 (ESRPs 1 and 2) regulate the splicing of FGFR-2 IIIc and IIIb.[35,36] ESRP-1 binds to the FGFR-2 auxiliary *cis*-element ISE/ISS-3, located in the intron between exon IIIb and IIIc, and this binding induces the expression of the FGFR-2 IIIb specific exon. Therefore, these splicing mechanisms may contribute to the reciprocal switching between FGFR-2 IIIb and IIIc isoforms. However, it is also possible that FGFR-2 IIIb and IIIc isoforms are modulated at a transcriptional level and/or through differential regulation of microRNAs that in turn regulate their selective expression.

Although endogenous levels of FGFR-2 IIIb were low in KLM-1 cells, engineered overexpression of FGFR-2 IIIc (causing a 5- to 13-fold increase in FGFR-2 IIIc levels) in these cells was associated with approximately a 40% decrease in the already low endogenous FGFR-2 IIIb levels. It is theoretically conceivable, therefore, that some component of the biological consequences of FGFR-2 IIIc overexpression might also be due to an indirect consequence of a slight lowering of endogenous FGFR-2 IIIb levels.

Studies of CSCs in pancreatic cancer have relied on sphere formation and SP assays and evaluation of CSC markers such as CD24, CD44, CD133, epithelial specific antigen (ESA), and CXCR4.[37–40] However, CSC markers in PDAC have not been accepted as definitive by all investigators. Furthermore, sphere formation in low-attachment culture plates is induced by FGF-2, which is a major ligand for FGFR-2 IIIc. We therefore used sphere formation and SP assays; both measures were increased in FGFR-2 IIIc-transfected cancer cells. It is not clear whether this effect is due to an intrinsic action of increased FGFR-2 IIIc levels or to activation of autocrine FGF-2-dependent pathways, given that FGF-2 is a major ligand for FGFR-2 IIIc. Irrespective of the mechanisms, these observations suggest that FGFR-2 IIIc may confer CSC-like characteristics to pancreatic cancer cells and may contribute to the maintenance of a CSC niche in PDAC.

Previously, FGFR-2 IIIc expression and epithelial-to-mesenchymal transition transformation have been reported to be closely related.[25,26] Most reports indicate that FGFR-2 IIIc induces epithelial-to-mesenchymal transition transformation, but in some reports FGFR-2 IIIc correlates with mesenchymal-to-epithelial transition.[22] In the present study, FGFR-2 IIIc stably transfected KLM-1 cells did not exhibit a spindle-like appearance or higher migration activity. However, further studies are necessary to delineate the role of FGFR-2 IIIc in epithelial-to-mesenchymal transition in pancreatic cancer cells. Given that FGFR-2 IIIc is not detected in normal cells in the pancreas, our findings raise the possibility that targeting FGFR-2 IIIc has a potential to suppress pancreatic cancer cell proliferation without exerting deleterious effects on normal cells. Thus, targeting FGFR-2 IIIc may allow for the development of novel therapeutic strategies to improve the survival of pancreatic cancer patients.

Acknowledgments

We thank Dr. Masahito Hagio for helpful discussion, Kiyoshi Teduka, Takenori Fujii, Taeko Suzuki, Yoko Kawamoto, and Kiyoko Kawahara (Nippon Medical School) for their excellent technical assistance and Dr. Shinichi Tsuchiya (Nippon Medical School Hospital) for preparing tissue blocks.

References

1. Lemal A, Siegel R, Ward E, Murray T, Xu J, Thun MJ: Cancer statistics, 2007. CA Cancer J Clin 2007, 57:43–66
2. Korc M: Role of growth factors in pancreatic cancer. Surg Oncol Clin N Am 1998, 7:25–41
3. Bardeesy N, DePinho RA: Pancreatic cancer biology and genetics. Nat Rev Cancer 2002, 2:897–909
4. Kornmann M, Beger HG, Korc M: Role of fibroblast growth factors and their receptors in pancreatic cancer and chronic pancreatitis. Pancreas 1998, 17:169–175
5. Cho K, Ishiwata T, Uchida E, Nakazawa N, Korc M, Naito Z, Tajiri T: Enhanced expression of keratinocyte growth factor and its receptor correlates with venous invasion in pancreatic cancer. Am J Pathol 2007, 170:1964–1974
6. Itoh N, Ornitz DM: Evolution of the Fgf and Fgfr gene families. Trends Genet 2004, 20:563–569
7. Itoh N: The Fgf families in humans, mice, and zebrafish: their evolutional processes and roles in development, metabolism, and disease. Biol Pharm Bull 2007, 30:1819–1825
8. Kornmann M, Ishiwata T, Matsuda K, Lopez ME, Fukahi K, Asano G, Beger HG, Korc M: IIIc isoform of fibroblast growth factor receptor 1

is overexpressed in human pancreatic cancer and enhances tumorigenicity of hamster ductal cells. Gastroenterology 2002, 123:301–313
9. Kornmann M, Lopez M, Beger H, Korc M: Expression of the IIIc Variant of FGF Receptor-1 Confers Mitogenic Responsiveness to Heparin and FGF-5 in TAKA-1 Pancreatic Ductal Cells. Int J Gastrointest Cancer 2001, 29:85–92
10. Liu Z, Ishiwata T, Zhou S, Maier S, Henne-Bruns D, Korc M, Bachem M, Kornmann M: Human fibroblast growth factor receptor 1-IIIb is a functional fibroblast growth factor receptor expressed in the pancreas and involved in proliferation and movement of pancreatic ductal cells. Pancreas 2007, 35:147–157
11. Liu Z, Neiss N, Zhou S, Henne-Bruns D, Korc M, Bachem M, Kornmann M: Identification of a fibroblast growth factor receptor 1 splice variant that inhibits pancreatic cancer cell growth. Cancer Res 2007, 67:2712–2719
12. Miki T, Bottaro DP, Fleming TP, Smith CL, Burgess WH, Chan AM, Aaronson SA: Determination of ligand-binding specificity by alternative splicing: two distinct growth factor receptors encoded by a single gene. Proc Natl Acad Sci USA 1992, 289:246–250
13. Eswarakumar VP, Lax I, Schlessinger J: Cellular signaling by fibroblast growth factor receptors. Cytokine Growth Factor Rev 2005, 16:139–149
14. Mohammadi M, Olsen SK, Ibrahimi OA: Structural basis for fibroblast growth factor receptor activation. Cytokine Growth Factor Rev 2005, 16:107–137
15. Yamanaka Y, Friess H, Buchler M, Beger HG, Uchida E, Onda M, Kobrin MS, Korc M: Overexpression of acidic and basic fibroblast growth factors in human pancreatic cancer correlates with advanced tumor stage. Cancer Res 1993, 53:5289–5296
16. Siddiqi I, Funatomi H, Kobrin MS, Friess H, Büchler MW, Korc M: Increased expression of keratinocyte growth factor in human pancreatic cancer. Biochem Biophys Res Commun 1995, 215:309–315
17. Ishiwata T, Friess H, Büchler MW, Lopez ME, Korc M: Characterization of keratinocyte growth factor and receptor expression in human pancreatic cancer. Am J Pathol 1998, 153:213–222
18. Kwabi-Addo B, Ropiquet F, Giri D, Ittmann M: Alternative splicing of fibroblast growth factor receptors in human prostate cancer. Prostate 2001, 46:163–172
19. Valve E, Martikainen P, Seppänen J, Oksjoki S, Hinkka S, Anttila L, Grenman S, Klemi P, Härkönen P: Expression of fibroblast growth factor (FGF)-8 isoforms and FGF receptors in human ovarian tumors. Int J Cancer 2000, 88:718–725
20. Drugan CS, Paterson IC, Prime SS: Fibroblast growth factor receptor expression reflects cellular differentiation in human oral squamous carcinoma cell lines. Carcinogenesis 1998, 19:1153–1156
21. Cha JY, Lambert QT, Reuther GW, Der CJ: Involvement of fibroblast growth factor receptor 2 isoform switching in mammary oncogenesis. Mol Cancer Res 2008, 6:435–445
22. Chaffer CL, Brennan JP, Slavin JL, Blick T, Thompson EW, Williams ED: Mesenchymal-to-epithelial transition facilitates bladder cancer metastasis: role of fibroblast growth factor receptor-2. Cancer Res 2006, 66:11271–11278
23. Marek L, Ware KE, Fritzsche A, Hercule P, Helton WR, Smith JE, McDermott LA, Coldren CD, Nemenoff RA, Merrick DT, Helfrich BA, Bunn PA Jr, Heasley LE: Fibroblast growth factor (FGF) and FGF receptor-mediated autocrine signaling in non-small-cell lung cancer cells. Mol Pharmacol 2009, 75:196–207
24. Yan G, Fukabori Y, McBride G, Nikolaropolous S, McKeehan WL: Exon switching and activation of stromal and embryonic fibroblast growth factor (FGF)-FGF receptor genes in prostate epithelial cells accompany stromal independence and malignancy. Mol Cell Biol 1993, 13:4513–4522
25. Baum B, Settleman J, Quinlan MP: Transitions between epithelial and mesenchymal states in development and disease. Semin Cell Dev Biol 2008, 19:294–308
26. Luqmani YA, Bansal GS, Mortimer C, Buluwela L, Coombes RC: Expression of FGFR2 BEK and K-SAM mRNA variants in normal and malignant human breast. Eur J Cancer 1996, 32A:518–524
27. Kawamoto M, Ishiwata T, Cho K, Uchida E, Korc M, Naito Z, Tajiri T: Nestin expression correlates with nerve and retroperitoneal tissue invasion in pancreatic cancer. Hum Pathol 2009, 40:189–198
28. Kawase R, Ishiwata T, Matsuda Y, Onda M, Kudo M, Takeshita T, Naito Z: Expression of fibroblast growth factor receptor 2 IIIc in human uterine cervical intraepithelial neoplasia and cervical cancer. Int J Oncol 2010, 36:331–340
29. Ishiwata T: Immunohistochemical and in situ hybridization analysis of lumican in colorectal carcinoma. Handbook of Immunohistochemistry and in Situ Hybridization of Human Carcinomas. Volume 2: Molecular Pathology, Colorectal Carcinoma, and Prostate Carcinoma. Edited by MA Hayat. Burlington, Elsevier Academic Press 2004, p. pp. 237–243
30. Vuillermoz B, Khoruzhenko A, D'Onofrio MF, Ramont L, Venteo L, Perreau C, Antonicelli F, Maquart FX, Wegrowski Y: The small leucine-rich proteoglycan lumican inhibits melanoma progression. Exp Cell Res 2004, 296:294–306
31. Seiden-Long I, Navab R, Shih W, Li M, Chow J, Zhu CQ, Radulovich N, Saucier C, Tsao MS: Gab1 but not Grb2 mediates tumor progression in Met overexpressing colorectal cancer cells. Carcinogenesis 2008, 29:647–655
32. Singh SK, Hawkins C, Clarke ID, Squire JA, Bayani J, Hide T, Henkelman RM, Cusimano MD, Dirks PB: Identification of human brain tumour initiating cells. Nature 2004, 432:396–401
33. Korc M, Friesel RE: The role of fibroblast growth factors in tumor growth. Curr Cancer Drug Targets 2009, 9:639–651
34. Yachida S, Jones S, Bozic I, Antal T, Leary R, Fu B, Kamiyama M, Hruban RH, Eshleman JR, Nowak MA, Velculescu VE, Kinzler KW, Vogelstein B, Iacobuzio-Donahue CA: Distant metastasis occurs late during the genetic evolution of pancreatic cancer, Nature 467:1114–1117
35. Warzecha CC, Sato TK, Nabet B, Hogenesch JB, Carstens RP: ESRP1 and ESRP2 are epithelial cell-type-specific regulators of FGFR2 splicing. Mol Cell 2009, 33:591–601
36. Warzecha CC, Shen S, Xing Y, Carstens RP: The epithelial splicing factors ESRP1 and ESRP2 positively and negatively regulate diverse types of alternative splicing events. RNA Biol 2009, 6:546–562
37. Immervoll H, Hoem D, Sakariassen PO, Steffensen OJ, Molven A: Expression of the "stem cell marker" CD133 in pancreas and pancreatic ductal adenocarcinomas, BMC Cancer 2008, 8:48
38. Li C, Heidt DG, Dalerba P, Burant CF, Zhang L, Adsay V, Wicha M, Clarke MF, Simeone DM: Identification of pancreatic cancer stem cells. Cancer Res 2007, 67:1030–1037
39. Ikenaga N, Ohuchida K, Mizumoto K, Yu J, Kayashima T, Hayashi A, Nakata K, Tanaka M: Characterization of CD24 expression in intraductal papillary mucinous neoplasms and ductal carcinoma of the pancreas. Hum Pathol 2010, 41:1466–1474
40. Mueller MT, Hermann PC, Heeschen C: Cancer stem cells as new therapeutic target to prevent tumour progression and metastasis. Front Biosci (Elite Ed) 2010, 2:602–613